The EMBO Journal (2006) 25, 302–311 | © 2006 European Molecular Biology Organization | All Rights Reserved 0261-4189/06
www.embojournal.org

THE EMBO JOURNAL

Dynamic study of the transition from hyaluronan- to integrin-mediated adhesion in chondrocytes

Miriam Cohen[1,2], Zvi Kam[1], Lia Addadi[2] and Benjamin Geiger[1,*]

[1]Department of Molecular Cell Biology, Weizmann Institute of Science, Rehovot, Israel and [2]Department of Structural Biology, Weizmann Institute of Science, Rehovot, Israel

Membrane-bound hyaluronan mediates the initial adhesive interactions between many cell types and external surfaces. In RCJ-P chondrocytes, such early contacts are mediated through a thick hyaluronidase-sensitive coat. The early adhesion is followed by integrin-mediated interactions and the formation of stable focal adhesions. During this process, the distance between the cell membrane and the surface is reduced from micrometers to few tens of nanometers. The transition from hyaluronan- to integrin-mediated adhesion was studied on glass surfaces by total internal reflection fluorescence microscopy. Hyaluronan-mediated adhesion precedes focal adhesions formation by 2–10 min. After these initial interactions, the pericellular hyaluronan remains sequestered into discrete pockets between the cell and the surface, which are a few hundreds nanometers thick and a few micrometers wide, and are flanked by focal adhesions. The hyaluronan coat facilitates the nucleation of small paxillin-rich contacts, which later mature into focal adhesions. These dynamic studies demonstrate that pericellular hyaluronan mediates initial cell–surface adhesion, and regulates the formation of focal adhesions.

The EMBO Journal (2006) **25,** 302–311. doi:10.1038/sj.emboj.7600960; Published online 12 January 2006
Subject Categories: cell & tissue architecture; structural biology
Keywords: cell adhesion; hyaluronan; integrins; quantum dots; TIRF

Introduction

Cell adhesion to the extracellular matrix (ECM) is a multi-step process that plays a key role in the regulation of cell proliferation, differentiation, motility, and survival (Geiger *et al*, 2001; Cohen *et al*, 2004; Zaidel-Bar *et al*, 2004). One of the earliest steps of ECM recognition by various cell types is mediated by a hyaluronan-based pericellular coat (Zimmerman *et al*, 2002; Cohen *et al*, 2004). Hyaluronan mediates early cell adhesion in a variety of physiological and pathological states, such as inflammation, wound repair, tumor invasion, angiogenesis, and during tissue morphogenesis (Turley *et al*, 1991; Savani *et al*, 2001; Toole, 2001). The initial attachment of lymphocytes and leukocytes to vascular endothelial cells (DeGrendele *et al*, 1996; Johnson *et al*, 2000; Nandi *et al*, 2004) and the adhesion and extravasation of T-cells (Siegelman *et al*, 2000) involve interaction of the hyaluronan receptor CD44 on the cells with pericellular hyaluronan on the endothelium (Johnson *et al*, 2000; Fries and Kaczmarczyk, 2003). The initial steps in metastasis require adhesion to the ECM and the endothelium, followed by transendothelial invasion. Metastatic cells express high levels of hyaluronan, which binds ECM components such as laminin as well as CD44 on endothelial cells (Draffin *et al*, 2004; Laurich *et al*, 2004).

Hyaluronan is a large linear glycosaminoglycan (D-*N*-acetylglucosamine-β-D-glucuronic acid), with a typical molecular weight of 10^6–10^7 Da. Due to the carboxyl group of the glucuronic acid, hyaluronan is negatively charged at physiological pH and forms hydrated gels at very low concentrations (<1%) (Laurent, 1987; Toole, 2004). Hyaluronan-dependent pericellular coats were observed around various cell types, including chondrocytes and fibroblasts, using particle exclusion assays (Lee *et al*, 1993). Due to the high hydration, hyaluronan pericellular coats are difficult to visualize, especially because dehydration, a mandatory step in conventional (non-cryo-)electron microscopy, inevitably reduces a hydrated pericellular coat to dispersed fibres.

Hydrated, 4.4 ± 0.7 μm-thick pericellular coats were observed around RCJ-P chondrocytes, and 2.2 ± 0.4 μm-thick coats were observed around A6 epithelial cells, using environmental scanning electron microscopy under fully hydrated conditions (Cohen *et al*, 2003). The thick coat of chondrocytes is probably organized as an entangled multi-layer of hyaluronan chains that can be peeled off the cells by sheer force, while the thinner coat of A6 epithelial cells was suggested to consist of a single layer, with each hyaluronan molecule directly anchored to the membrane (Cohen *et al*, 2004). Adhesion of chondrocytes and A6 epithelial cells involves interaction of the pericellular hyaluronan with the surface (Hanein *et al*, 1993, 1994; Zimmerman *et al*, 2002; Cohen *et al*, 2003). These interactions are specific, and depend on the organization of hyaluronan in the pericellular coat. The hyaluronan coat of A6 epithelial cells mediates rapid adhesion to specific crystal surfaces (Hanein *et al*, 1993, 1994; Zimmerman *et al*, 2002) as well as conventional substrates, and its removal by hyaluronidase blocks or slows down the adhesion of these cells to a variety of substrates (Hanein *et al*, 1993, 1994; Zimmerman *et al*, 2002). Interestingly, hyaluronan can also block adhesive interactions, when present on both the cell surface and the adhesion substrate (Zimmerman *et al*, 2002). In contrast to the rapid interaction of A6 cells, the thick entangled multilayered pericellular coat around chondrocytes mediates 'soft contacts' with the surface, allowing cell drifting following the application of an external sheer force (Cohen *et al*, 2003, 2004).

*Corresponding author. Department of Molecular Cell Biology, Weizmann Institute of Science, Rehovot 76100, Israel.
Tel.: +972 8 934 3910 or 4069; Fax: +972 8 946 5607;
E-mail: benny.geiger@weizmann.ac.il

Received: 22 August 2005; accepted: 6 December 2005; published online: 12 January 2006

Hyaluronan-mediated adhesion thus initiates when the cell membrane is separated from the surface by a few micrometers. The following stage of adhesion involves integrin interaction with their ligands. Integrins are transmembranal heterodimers of α and β subunits, which bind to ECM components such as fibronectin and vitronectin (Zamir and Geiger, 2001; Hynes, 2002) and form the intracellular membrane interface to the actin cytoskeleton (Critchley, 2000). Following integrin–ECM interactions, an adhesion complex is formed, containing multiple molecules, including paxillin, vinculin, and talin (Petit and Thiery, 2000; Geiger *et al*, 2001; Zamir and Geiger, 2001; Hynes, 2002). Once focal adhesions, the prototypic form of integrin-mediated adhesions, are established, the cell membrane is typically separated by only a few tens of nanometers from the substrate, ranging from ~15 nm (Curtis, 1964) to ~50 nm (Iwanaga *et al*, 2001), suggesting that before reaching this proximity the pericellular hyaluronan must be modified or removed by the cells.

Here we study the dynamics of the transition from the initial 'soft' hyaluronan-mediated adhesion to the formation of tight integrin-mediated contacts. In order to follow the sequence of molecular events involved in these adhesive interactions, we took two-color total internal reflection fluorescence (TIRF) (Reichert and Truskey, 1990) time-lapse movies of cells expressing paxillin–GFP, with the hyaluronan coat labeled by quantum dots (QDs). The dynamic relations between hyaluronan and focal adhesions formation were investigated by single-cell analysis of early cell–matrix interactions, with time resolution of seconds-to-minutes.

Results

Hyaluronan-mediated adhesion precedes fibronectin-mediated adhesion

Characterization of the initial interactions between the cells and the underlying surfaces requires specialized techniques that enable visualization of the cell–surface interface at high temporal and spatial resolution. The primary technique of choice, in this study, was TIRF microscopy (Reichert and Truskey, 1990). In TIRF, a laser beam enters the sample coverslip at a shallow angle such that it is fully internally reflected from the interface between glass and sample buffer. This produces an evanescence wave, which decays exponentially as a function of distance from the glass surface. As a result, fluorescence is effectively excited from the sample only in a region of about half the wavelength, namely, ~240 nm from the interface, using the illumination system used in our experiments. The cell–substrate interface may thus be observed, avoiding background fluorescence from deeper regions in the cell body.

In order to study the transition from hyaluronan- to integrin-mediated adhesion, a line of chondrocytes, stably expressing the fusion protein paxillin–GFP, was prepared. This protein is normally targeted to early stages of cell–matrix focal adhesion assembly (Zamir and Geiger, 2001). The hyaluronan pericellular coat of the same cells was labeled with biotinylated hyaluronan-binding protein (bHABP), bound to streptavidin-conjugated QDs. The double fluorescence labeling allowed simultaneous monitoring of the hyaluronan pericellular coat and of focal adhesions. Double-labeled cells were seeded on thin glass culture dishes precoated with 15% serum. Time-lapse movies were recorded using two-color TIRF microscopy, starting 1 min after plating the cells, and collecting images every 15 s for 75 min (see Supplementary Movie 1).

In all, 17 cells from the TIRF movies were examined frame-by-frame for the appearance of QD and paxillin. Hyaluronan interactions with the surface are indicated by the appearance of QDs within the TIRF field, which occurred in all cells minutes before paxillin became visible. Specifically, this phase of exclusively hyaluronan-mediated cell–substrate interactions lasted at least 2 min and up to 10 min before paxillin appeared in the TIRF field (2.9 min mean value). The onset of paxillin appearance was defined by a persistent increase in the pixel intensity of paxillin–GFP above background (Figure 1F). Interestingly, after the first appearance of paxillin sites, definite paxillin-containing structures formed within 30 s, indicating that the formation of stable adhesion complexes following the formation of the first direct physical contact is relatively fast (sub-minute) (Figure 1F). While it appears that paxillin-rich focal adhesions are induced following interactions with the substrate, we cannot exclude the possibility that paxillin is recruited to the membrane even before the cell membrane attaches to the surface, which might facilitate formation of focal adhesions.

In one of the cells (see Supplementary Movie 1), the first QDs (Figure 1A, arrowheads) appear 10 min before paxillin–GFP structures become visible (Figure 1B, arrow). Definite focal adhesions are formed after an additional 2 min, and the cell rapidly spreads (Figure 1C). Similar results were obtained for cells seeded on glass surfaces precoated with 10 μg/ml fibronectin or 100% serum. In both cases the QDs preceded the appearance of paxillin-containing structures by more than 1 min, indicating that the nature of the surface-bound ECM does not affect the order of formation of hyaluronan- and integrin-mediated adhesions. It was noted that the formation of hyaluronan-mediated adhesions, as determined by QDs appearance, was somewhat delayed on the fibronectin-coated surfaces (compared to serum-coated surfaces), suggesting that fibronectin might reduce the interaction of the hyaluronan coat with the surface (Supplementary Figure 1).

Lateral movement within the hyaluronan gel

The hyaluronan pericellular coat of chondrocytes was shown to be approximately 5 μm thick (Cohen *et al*, 2003), whereas the distance between the cell membrane and the surface in focal adhesions is only a few tens of nanometers. Thus, the hyaluronan layer needs to be reduced (at least locally) by a factor of 40–100, or removed from the cell–substrate interface, to enable focal adhesion formation. Examination of QDs lateral movement showed, however, no directional translocation of QDs, implying that the hyaluronan coat is not displaced to the cell periphery during focal adhesion formation (Figure 1D). As the QDs occupy less than 0.05% of the volume of the pericellular hyaluronan coat (experimental value), they are not likely to significantly affect the lateral displacement of the coat. QDs that can be tracked only in a small number of frames (due to changing heights) may appear to have some directional movement, but even in these cases they do not display any preferential movement toward the cell periphery (Figure 1E). QDs persisting for a large number of frames move randomly within regions of a few to 15 μm^2, implying that hyaluronan remains trapped

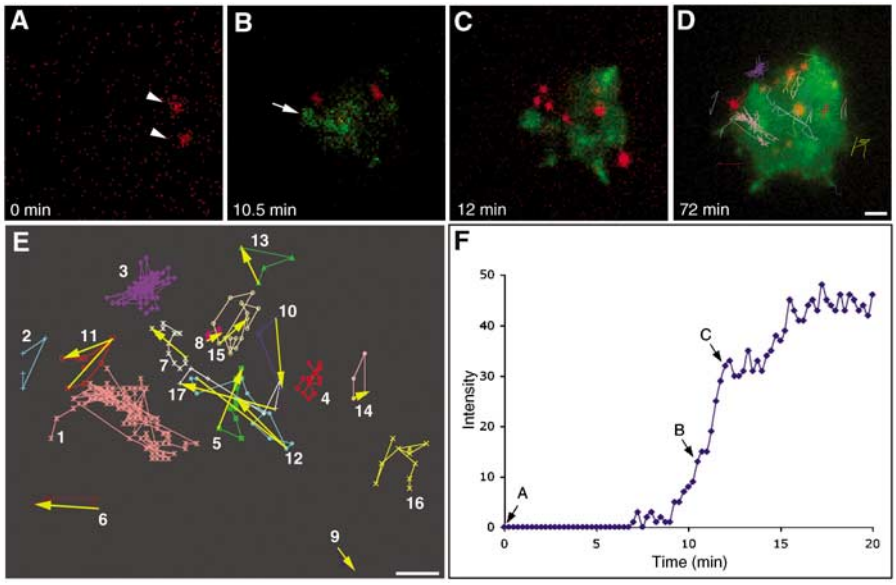

Figure 1 Appearance of hyaluronan-bound QDs precedes integrin-mediated adhesion by at least 2–10 min. A stable line of chondrocytes, RCJ-P, expressing paxillin–GFP fusion protein was labeled with biotinylated hyaluronan-binding protein and streptavidin-conjugated QDs. Labeled cells were seeded on a glass bottom culture dish and time-lapse movies were immediately taken using two-color TIRF microscopy, acquiring an image every 15 s for 75 min (see Supplementary Movie 1). (**A**) QDs become visible 2.5 min after cell plating, marked here as time zero (red, arrowheads). (**B**) Paxillin–GFP became visible only 10.5 min later (green, arrow). (**C**) Definite paxillin-containing focal adhesions appear only after additional 1.5 min. (**D**) Tracking of QDs lateral movement (colored tracks) shows no directional movements of QDs, implying that hyaluronan is not being displaced towards the cell periphery during cell spreading and focal adhesion formation. (**E**) A chart depicting QDs tracks. The numbers indicate the order of QDs appearance in the movie. (**F**) Intensity plot of a paxillin–GFP-containing structure (marked with an arrow in B), showing a rapid increase in intensity as soon as the structure becomes visible. Arrows in (F) mark the structure intensity in the corresponding movie frames shown in (A), (B), or (C). Scale bar = 2 μm.

in 'pockets' under the cells rather than being pushed to the cell periphery.

Vertical movement of QDs

In the TIRF field, movements in the vertical direction lead to exponential decay in light intensity, such that particles close to the glass surface have the highest intensity. The intensity decays sharply when moving away from the glass and disappears when the QDs are located at distances >240 nm from the glass. However, changes in fluorescence intensity may be attributed not only to vertical movement of the QDs but also to blinking (Shimizu *et al*, 2002). To assess the extent of vertical movements of the hyaluronan-bound QDs, we measured the QDs intensity during the movie and determined the frequency of intensity fluctuations. The measured QDs intensities are depicted here using 3D graphs; the cell periphery is outlined in red, whereas the heights of the peaks represent QD intensity (Figure 2 and Supplementary Movie 2). Individual QDs are represented with distinct colors.

QDs display fast dynamics during the first 10 min of adhesion, before the formation of defined paxillin-containing structures (illustrated in four sequential frames from Supplementary Movie 2; Figure 2A and B). Eight different QDs are visible, each in one of these sequential frames, with the exception of the yellow peak that is visible in two frames. As the blinking probability of QDs calculated for our experiment (exposure time of 500 ms) according to Shimizu *et al* (2002) is 1:10, it is unlikely that all eight QDs disappear due to blinking. As cell spreading progresses, more QDs become visible: for example, 16 QDs appear within four sequential frames 21–21.75 min after seeding (Supplementary Movie 2), suggesting that a larger amount of hyaluronan accumulates within a volume of thickness ~240 nm (TIRF range) from the glass substrate. This could result from collapse of the hyaluronan coat under the cell (Figure 2C and D). Furthermore, the QDs are less dynamic at late time points, compared to the first 10 min of adhesion: seven QDs (44%) appear in at least two frames, but nine QDs (56%) still appear only in one frame. The fluctuation in QDs fluorescence intensity was again almost an order of magnitude faster than anticipated from the blinking probability. Based on these considerations, we conclude that QDs disappearance represents vertical displacements of 240 nm or more of the hyaluronan-bound QDs. This implies that part of the hyaluronan pericellular coat remains encapsulated in subcellular domain pockets with thicknesses >240 nm, during and even after spreading (Figure 2C and D). These pockets are concentrated in areas flanked by focal adhesions, but not densely populated by focal adhesions in their interior.

Hyaluronan redistribution under the cells during spreading

In an effort to follow the fate of hyaluronan before, during and after formation of focal adhesions, we have recorded the history of QDs lateral movements throughout the entire spreading process. To mark the space occupied by hyaluronan, the appearance of each QD was represented by a colored pixel, and all pixels were plotted in cumulative manner, such that all the positions where a QD appeared at any time are marked with a colored pixel. Different colors were assigned for QDs detected within specific time windows, whereas white pixels correspond to paxillin-containing struc-

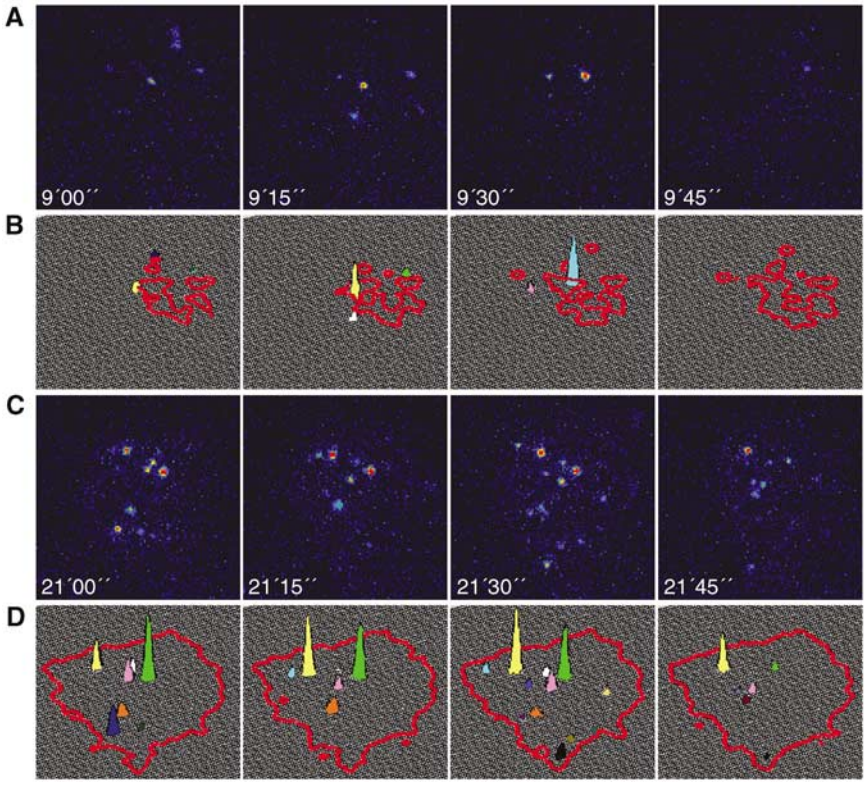

Figure 2 Vertical movement of QDs. QDs moving more than 200 nm away from the glass surface exit the TIRF excitation range and disappear. Images were acquired every 15 s and the exposure time was 500 ms (under such conditions, QDs blinking probability is ~1:10). (**A, C**) Four sequential frames from a TIRF movie; QDs are shown in intensity scale, where higher intensity is represented by warmer colors. (**B, D**) The fluctuations in QDs intensity are depicted using 3D graphs; the cell periphery is outlined in red and QD intensity by the colored peaks. During the first 10 min of adhesion QDs are very dynamic, as illustrated in four sequential frames from a movie (A and B). When the cell is spreading QDs are restrained, implying that the hyaluronan pericellular coat remains localized under the cells after spreading (C and D).

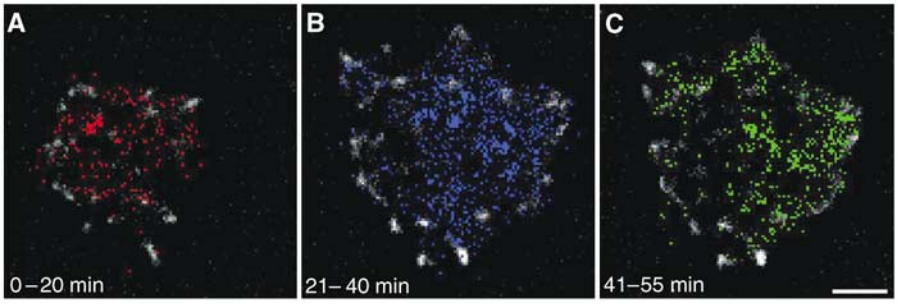

Figure 3 Reorganization of QDs under spreading cells. The area under the cells that is covered with hyaluronan is indicated by the history of QDs translational movements in the XY plane. Each appearance of a QD is represented by a colored pixel. All pixels are plotted in a cumulative manner such that all the coordinates in which QDs appeared are marked with a colored pixel. Paxillin-containing structures are white. (**A**) During the first 20 min, QDs appear all over the cell-surface interface; (**B**) 21–40 min after seeding, additional QDs accumulate under the cell, displaying an increasingly nonuniform distribution. (**C**) As the cell continues to spread (41–55 min), QDs becomes confined to discrete areas under the cell, in the area located between focal adhesions, and their movement in the *XY* plane become restrained. Scale bar = 5 μm.

tures (Figure 3 and Supplementary Movie 3). QDs detected within the first 0–20 min after seeding were distributed under the cell more or less homogeneously (Figure 3A). At later stages, concomitantly with cell spreading and increased focal adhesion formation, QDs became progressively clustered in confined pockets and their movement in the XY plane was restrained (Figure 3C).

A similar reorganization of hyaluronan under spreading chondrocytes was observed using Quantomix QX^{TM} chambers, designed for 'wet SEM' analysis (Gileadi and Sabban, 2003). A thin membrane, to which the cells can adhere, seals these chambers, such that, following fixation, the sample can be observed in the scanning electron microscope (with the membrane side facing the electron gun), while the cells remain immersed in water. The electron beam penetrates through the membrane reaching the cells. Chondrocytes were labeled with bHABP and streptavidin-gold, and seeded in QX^{TM} capsules for 5, 10, 20 and 30 min, before fixation. Gold particles are visible on the ventral side of the cell membrane (Figure 4, white particles). The beam penetration

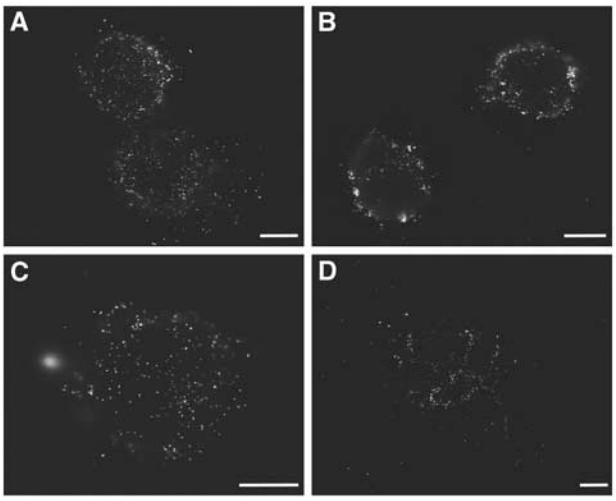

Figure 4 Reorganization of hyaluronan under the cell during spreading. Hyaluronan reorganization is observed by scanning electron microscopy using QX^{TM} capsules. RCJ-P cells were labeled with biotinylated hyaluronan-binding protein and streptavidin-conjugated colloidal gold, and seeded in a QX^{TM} capsules for 5, 10, 20, and 30 min before fixation. Gold particles are visible on the ventral side of the cell membrane (white particles). (**A**) Gold particles are scattered evenly under the cells 5 min after seeding. (**B**) After 10 min the gold particles appear more organized within discrete areas under the cells. (**C, D**) At 20 and 30 min after seeding, the gold particles become increasingly clustered in compartments under the cells. Scale bars = 5 μm.

through QX^{TM} capsules is estimated to be 2–3 μm (Gileadi and Sabban, 2003). Gold particles located at a distance >3 μm from the membrane appear unfocused. This property gives a qualitative dimension of depth to the sample. In agreement with the TIRF observations, gold particles are scattered evenly under the cells 5 min after seeding (Figure 4A), but after 10 min the gold particles appear more organized (Figure 4B). At 20 and 30 min after seeding, the gold particles become clustered under the cells in well-defined pockets (Figure 4C and D, respectively).

CD44 is excluded from paxillin-containing structures

Formation of paxillin-containing adhesions in areas devoid of QDs suggested that these newly formed structures are spatially distinct from hyaluronan adhesions (Figure 1A). In order to further characterize the spatial relationships between these adhesions, chondrocytes expressing paxillin–GFP were fixed 20 min after seeding on uncoated glass, and labeled for the hyaluronan receptor CD44, vinculin, and phosphotyrosine (Figure 5B). The CD44 localization is negatively correlated with paxillin–GFP (Figure 5B, first row), in agreement with the QDs localization. This negative correlation between QDs and paxillin–GFP was also observed on serum-coated (data not shown) and fibronectin-coated glass surfaces (Figure 5A). Both the focal adhesion molecules vinculin and phosphotyrosine colocalize with paxillin–GFP in a typical pattern of focal adhesions (Zamir *et al*, 1999) (Figure 5B, second and third rows, respectively). Similar results were obtained for cells that were seeded 10 min before fixation (data not shown). We conclude that there are two distinct structures that mediate the early stages of cell–surface adhesion. The first structure formed, which mediates the initial surface interactions, contains hyaluronan and is CD44-bound. Paxillin- and vinculin-rich focal adhesions form at a later time and are independent of the first structures, so much so that they are reciprocally exclusive.

Focal adhesion formation is modulated by hyaluronan

The hyaluronan pericellular coat forms a micrometer-thick barrier between the cell membrane and the adhesive surface. This layer can thus modulate the extent, pattern, and dynamics of cell–matrix adhesion. In order to study the effect of hyaluronan on focal adhesion formation, chondrocytes expressing paxillin–GFP were treated with hyaluronidase (from bovine testes or from *Streptomyces hyalurolyticus*), an enzyme that cleaves hyaluronan. Upon this enzymatic treatment, the hyaluronan pericellular coat is reduced below detection levels. This was established using several independent microscopy methods, including environmental scanning electron microscopy and particle exclusion assay (Cohen *et al*, 2003), and direct labeling with bHABP and streptavidin-conjugated CY3 (data not shown). Furthermore, hyaluronidase treatment inhibits or slows down the hyaluronan-dependent adhesion of cells to various substrates (Hanein *et al*, 1993, 1994; Zimmerman *et al*, 2002; Cohen *et al*, 2003). The treated cells were then seeded on glass plates and their adhesion and spreading were monitored using time-lapse video microscopy under TIRF illumination. Images were collected every 15 s for 15 min, starting 1 min after seeding. The formation of paxillin-containing structures in hyaluronidase-treated cells was compared with their formation in untreated cells (Supplementary Movie 4).

In the presence of pericellular hyaluronan, the cells form many small paxillin-containing structures all over the contact area (Figure 6A and E). Hyaluronidase-treated cells form fewer dot-like paxillin-mediated adhesions, which are primarily located at the cell periphery (Figure 6B and E). These differences appear to be transient, since upon longer incubation (e.g. 60 min after seeding) both untreated and hyaluronidase-treated cells form large apparently indistinguishable focal adhesions at the cell periphery (Figure 6C and D, respectively).

In order to visualize the dynamics of focal adhesion formation and reorganization, temporal fluorescence ratio image (FRIT) analysis (Zamir *et al*, 2000) was performed based on these TIRF movies (Figure 7). The FRIT images indicate that cells with intact pericellular hyaluronan form many new paxillin-containing structures (blue pixels in Figure 7A) that are visible in each of the frames (taken at 15-s intervals). Once formed, these structures remain stable (yellow pixels; Figure 7A). In contrast, hyaluronidase-treated cells initially form few central paxillin-containing structures, which migrate to the periphery or dissolve and disappear (red), while additional paxillin-containing structures appear, mainly at the cell periphery, about a minute after the first structures are formed (Figure 7B). We conclude that the hyaluronan pericellular coat promotes the nucleation of nascent adhesions between the cell and the substrate and stabilizes these adhesions. Hyaluronidase-treated cells adhere to the substrate less efficiently, forming fewer adhesion sites, which, once formed, grow rapidly to large sizes at the cell periphery.

Discussion

In this study, we explored the dynamic relations between early hyaluronan-mediated adhesion of cultured chondro-

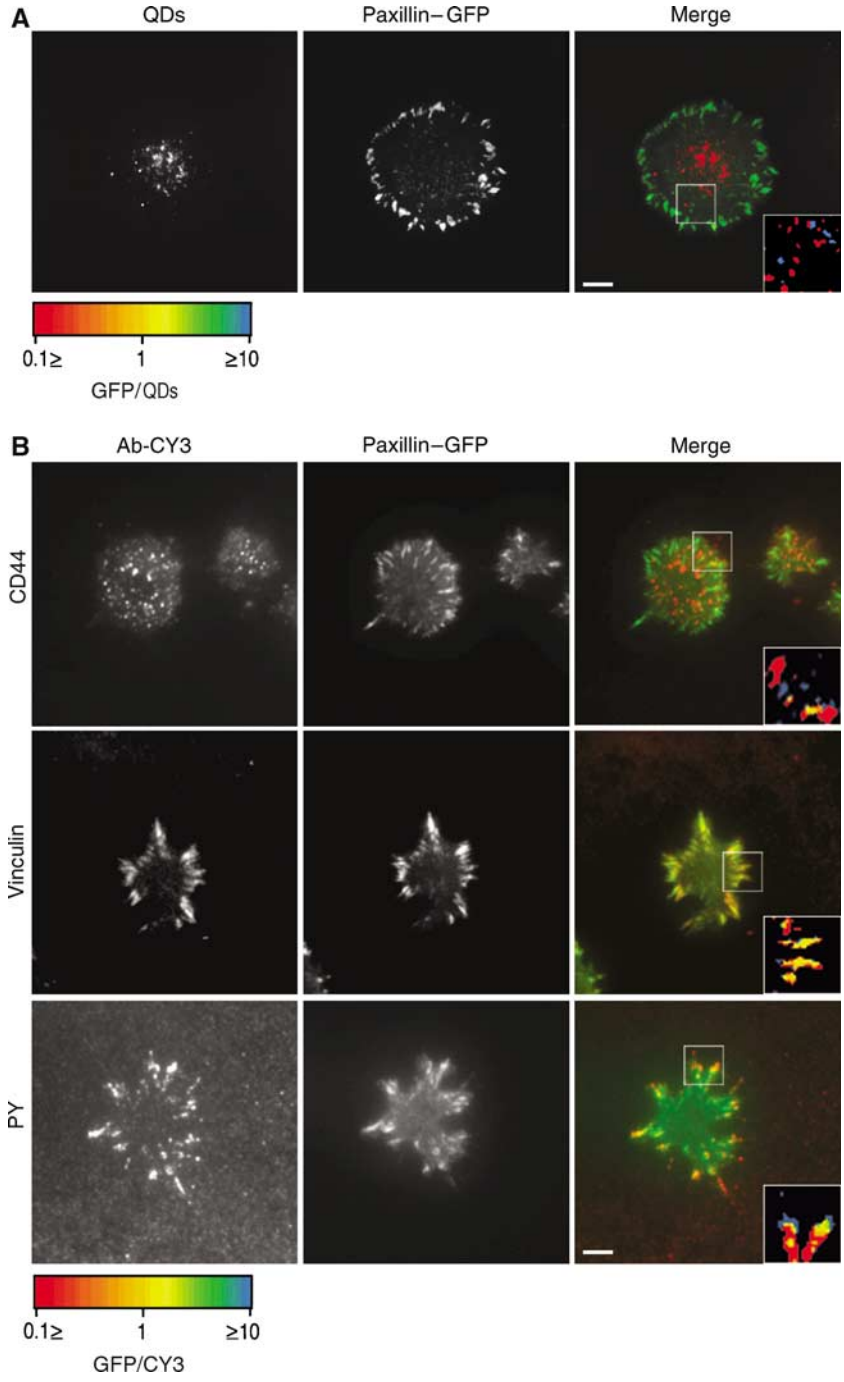

Figure 5 Hyaluronan-bound QDs and CD44 do not colocalize with paxillin-containing structures. (**A**) RCJ-P chondrocytes stably expressing paxillin–GFP were labeled with biotinylated hyaluronan-binding protein and streptavidin-conjugated QDs, seeded on fibronectin-coated glass (10 μg/ml) and incubated for 20 min before fixation. Left: QDs; middle: paxillin–GFP; right: merged image. (**B**) RCJ-P chondrocytes stably expressing paxillin–GFP were seeded on uncoated glass, incubated for 20 min, fixed and immunolabeled for CD44, vinculin and phosphotyrosine. Left: antibody-CY3 expression; middle: paxillin–GFP; right: merged image. Insets: fluorescence ratio analysis of the areas marked with a box. Red: structures with high paxillin–GFP/Ab-CY3 or paxillin–GFP/QDs ratio, Blue: structures with low paxillin–GFP/Ab-CY3 or paxillin–GFP/QDs ratios. Yellow: paxillin–GFP/Ab-CY3 or paxillin–GFP/QDs, normalized ratio = 1. Scale bar = 5 μm. (A, B) The localization of QDs and of the hyaluronan receptor CD44 is negatively correlated with paxillin–GFP. (B) Vinculin colocalizes with paxillin,phosphotyrosine colocalizes with the tips of paxillin-containing structures.

cytes and the formation of integrin-mediated contacts. Chondrocytes, the cartilage-forming cells, are surrounded by a several micrometer-thick pericellular coat (Lee *et al*, 1993; Knudson and Loeser, 2002; Cohen *et al*, 2003) comprised of a hyaluronan scaffold, decorated with aggrecan and additional link proteins (Knudson and Loeser, 2002). This thick pericellular coat mediates, initially, 'soft contacts' of chondrocytes with the substrate (Cohen *et al*, 2003), which are sensitive to external mechanical perturbation. The TIRF measurements presented here indicate that, during this early phase, lasting 2–10 min, no paxillin-containing structures are formed, and adhesion appears to be mediated by the

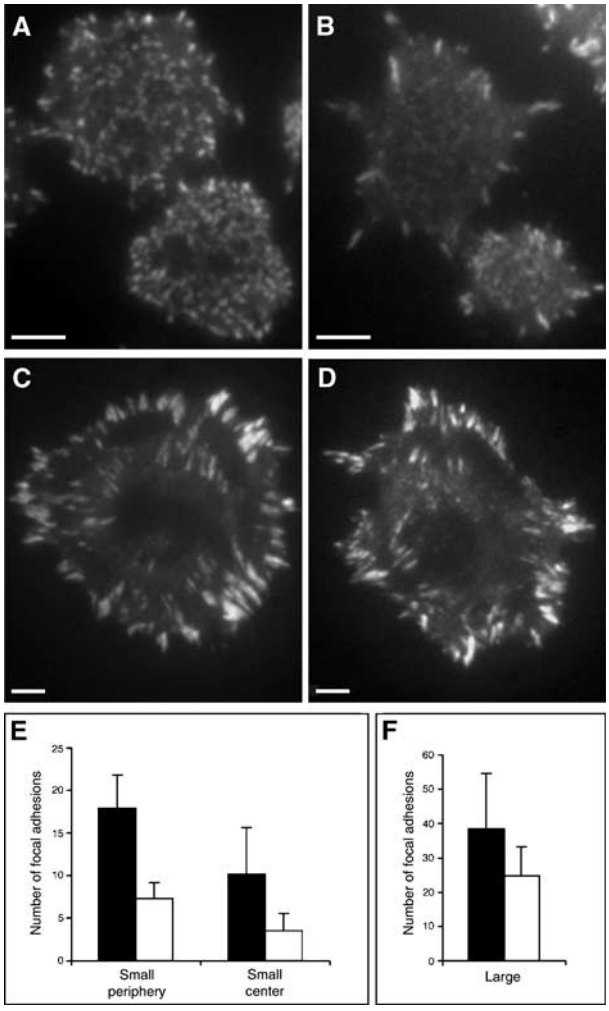

Figure 6 The pericellular hyaluronan coat modulates the formation of paxillin-containing adhesion structures. (**A**) A line of RCJ-P chondrocytes, stably expressing paxillin–GFP, 15 min after plating forms many small paxillin-containing dot-like adhesions throughout the ventral cell surface. (**B**) Hyaluronidase treatment of the same cells leads to a major reduction in the formation of such adhesive structures at the cell center, and most of the adhesions are confined to the cell periphery. When the cells are allowed to spread for 60 min, both untreated (**C**) and hyaluronidase-treated cells (**D**) form large focal adhesions at the cell periphery. (**E, F**) The number of paxillin-containing adhesions in hyaluronidase-treated (□) and untreated cells (■) located at the cell center and at the cell periphery following 15 min of adhesion. (E) Hyaluronidase-treated cells develop significantly less small paxillin-containing adhesions, both in the cell center ($P<0.01$) and cell periphery ($P<0.001$) compared to untreated controls. (F) Most of the paxillin-containing structures formed in hyaluronidase-treated cells are large and located at the cell periphery. Data represent the means ± s.d. of three independent experiments; a total of 750 paxillin-containing structures was examined. Statistical analysis was derived from Student's *t*-test. Scale bars = 5 μm.

pericellular coat only (Figure 1). Once the cell membrane enters the ~240 nm-thick 'TIRF zone', integrin adhesions are formed, and paxillin is recruited to the nascent adhesions within seconds thereafter (Zaidel-Bar *et al*, 2004). These adhesion structures tether the cells to the surface with much greater force compared to the hyaluronan-based adhesions. Cells with only two or three visible paxillin-containing structures, are resistant to mechanical perturbations, such as shear stress, that are sufficient for detaching cells that are tethered to the surface via the hyaluronan coat (Cohen *et al*, 2003). For integrin molecules to be able to bind their respective ligands (Hynes, 1992; Martin *et al*, 2002), the micrometer-thick hyaluronan coat must be modified by the cell so as to allow the formation of direct integrin–ligand interactions. At least three mechanisms for modifying the hyaluronan coat may be considered: (1) lateral displacement of hyaluronan from the cell–substrate interface to the cell periphery, (2) enzymatic degradation or endocytosis of the pericellular coat, (3) collapse of the pericellular coat on the substrate to a thickness that permits the formation of integrin-mediated adhesions (Cohen *et al*, 2004). Monitoring the fate of hyaluronan during the spreading process indicated that there is no apparent directional displacement of hyaluronan from underneath the cell (Figure 1E). Rather, hyaluronan accumulates at the cell–surface interface and remains trapped there throughout spreading, accumulating in large pockets, a few square micrometers wide and several hundreds nanometres thick (Figures 2–4). These regions resemble in their dimension and overall distribution the broad areas located between focal adhesions, which were defined, based on interference reflection microscopy, as 'close contacts' (Izzard and Lochner, 1976, 1980). Close contacts are highly dynamic structures whose dimensions are strongly affected by ambient pH, such that reduction of pH in the medium to below 6.2 results in extension of close contacts area, combined with decrease in cell–substrate separation (Avnur and Geiger, 1981). Interestingly, grafted hyaluronan is also sensitive to pH and ion concentration (Albersdorfer and Sackmann, 1999), as expected from polyelectrolyte gels. The role of close contacts has not been elucidated, yet they appear to be interspaced between focal adhesions and precede their formation, similar to the behavior of the hyaluronan-based contacts observed here.

What is the role of the transient, hyaluronan-mediated adhesions? The results presented here, together with those of previous studies (Cohen *et al*, 2003), suggest that the hyaluronan pericellular coat greatly facilitates the nucleation of integrin adhesion formation both on serum-coated, fibronectin-coated and uncoated glass surfaces. Hyaluronan-mediated interaction with these surfaces precedes the formation of focal adhesions by a few minutes, and the focal adhesions formed do not colocalize with CD44 and hyaluronan-bound QDs (Figures 3 and 5). This implies that the two adhesion systems involved are functionally inter-related, but spatially segregated. Hyaluronan mediates specific recognition of the adhesive substrate, tethering of the cell membrane to the surface, and brings the integrin receptors in close proximity to their matrix-associated ligands (Hanein *et al*, 1993, 1994; Zimmerman *et al*, 2002).

Indeed, live cell monitoring of focal adhesion development in the presence and absence of surface hyaluronan using TIRF microscopy shows that the hyaluronan coat nucleates the formation of multiple dot-like, paxillin-containing structures throughout the entire ventral cell surfaces (Figure 6A and E). Removal of the pericellular hyaluronan coat suppressed the formation of such adhesions (Figure 6B and E), and delayed the formation of focal adhesions at the cell periphery (see Supplementary Movie 1). It is conceivable that, following the establishment of the first hyaluronan–substrate contacts, the hyaluronan layer collapses, either due to its binding to the surface or as a result of cell-induced

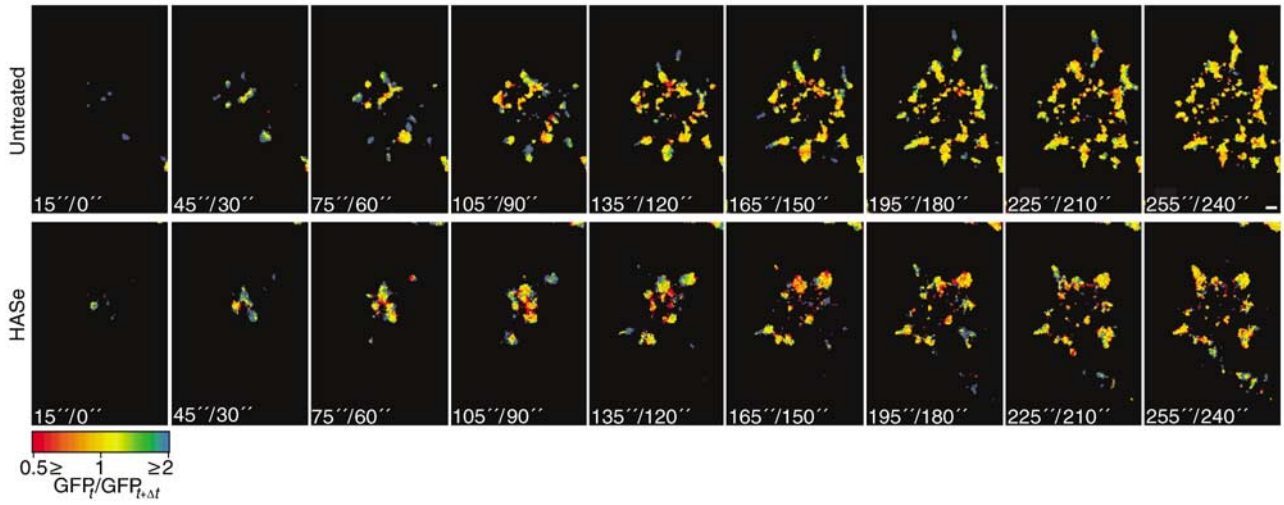

Figure 7 Temporal FRIT analysis of paxillin–GFP, in the presence or absence of pericellular hyaluronan. The dynamic behavior of paxillin–GFP in RCJ-P cells is shown here by the FRIT analysis of pairs of images taken in 15-s intervals, using TIRF microscopy. The spectrum scale indicates the value of the ratio in a range from 0.5 (red) to 2 (blue), with yellow indicating equal normalized intensities (FRIT = 1). Thus blue indicates a new structure, red indicates a structure that has disappeared and yellow indicates structures that remained constant. (**A**) Untreated cells continuously form new structures during first 4 min of attachment (blue). On average, 4.63 ± 1.17 new structures are formed every 30 s. (**B**) Hyaluronidase-treated cells form few structures at the center that rapidly disappear while new structures form at the periphery. Overall, 3.17 ± 1.13 new structures are formed every 30 s, which is significantly lower than in untreated cells ($P < 0.0001$). A total of five cells from each experiment were examined. Statistical analysis was based on Student's *t*-test. Scale bar = 2 μm.

changes in its immediate environment, reducing the gap between the cell membrane and the matrix (Cohen *et al*, 2004). This would allow integrins to bind to their specific adhesive ligands and trigger the initiation of focal adhesion formation (Geiger and Bershadsky, 2002). The mechanism for the collapse of the hyaluronan coat, however, has not yet been established.

The mechanism for the transition between hyaluronan- and integrin-mediated adhesion is not clear. In a conceivable scenario hyaluronan-mediated tethering may also function in the transmission of adhesion-mediated signals, in addition to its mechanical role in cell adhesion. CD44, which is a major hyaluronan receptor (Knudson and Loeser, 2002), is a transmembrane molecule, whose cytoplasmatic domain interacts with actin-associated ERM proteins (ezrin, radixin, moesin), as well as with ankyrin, which interacts with the cytoskeletal component spectrin (Ponta *et al*, 2003). These interactions of the CD44 tail are phosphorylation dependent and were reported to involve the activation of Rho signaling (Bourguignon *et al*, 1999; Ponta *et al*, 2003). Furthermore, engagement of CD44 was reported to promote integrin activation (Fujisaki *et al*, 1999; Khan *et al*, 2004). The mutual exclusive distributions of focal adhesion components and CD44 (Figure 5), as well as the distinct distributions of hyaluronan (decorated with QDs) and focal adhesions (decorated with GFP-paxillin), suggest that the crosstalk between these two adhesion systems is based on long-range interactions rather than on direct coupling of the adhesion receptors involved. These data, while being rather indirect and often circumstantial, raise the attractive possibility that interaction of the hyaluronan coat with the external surface might be 'sensed' by the cell, and trigger signaling events, minutes before integrin becomes engaged. This would provide an attractive model for 'remote mechanosensitivity', through which cells may 'sense' tethering to an external matrix from a distance of a few micrometers and respond to it by activating adhesion.

Materials and methods

Cell culture

RCJ-P chondrocytes (rat chondrocytes from fetal calvaria, batch 15.01.98; Prochon Biotech, Rehovot, Israel) were cultured at 37°C in a humidified atmosphere of 5% CO_2 in air in α-minimum essential medium (Biological Services, The Weizmann Institute) supplemented with 15% fetal calf serum (Biolab Ltd, Jerusalem, Israel).

Immunochemical reagents

The primary antibodies used in this study included: rabbit anti-phosphotyrosine (PT40, kindly provided by Israel Pecht and Arie Licht, The Weizmann Institute), monoclonal antibody anti-vinculin (clone hVin-1, Sigma Chemical Co., St Louis, MO), and rabbit anti-CD44 (HCAM, H-300, Santa Cruz Biotechnology, Inc., Santa Cruz, CA). Second antibodies used in this study were Cy3-conjugated goat anti-mouse IgG and Cy3-conjugated goat anti-rabbit IgG (Jackson ImmunoResearch Laboratories Inc., West Grove, PA).

Fusion protein construction

Full-length human paxillin was subcloned into pEGFP-C3 vector (Clontech, Palo Alto, CA). The fusion protein (paxillin–GFP) was then cut with *Sna*BI and *Sal*I restriction enzymes and ligated into pBABE at the multi-cloning site. RCJ-P cells were infected with the fusion construct, clones were isolated by fluorescence-activated cell sorter (Flow Cytometry Unit, The Weizmann Institute), and a single clone was then selected.

Immunofluorescence staining

Cells were seeded on tissue culture dishes and allowed to adhere for 20 min. They were then fixed–permeabilized with 3% paraformaldehyde (MERCK, Darmstadt, Germany), 0.5% Triton X-100 (Sigma) in PBS for 2 min, and post-fixed with 3% paraformaldehyde for 25 min. The cells were then washed with PBS and stained with primary antibodies for 45 min. For anti-HCAM staining, the permeabilization step was skipped. After washing with PBS, the cells were stained with secondary antibodies. Finally, the cells were washed with PBS and examined by TIRF microscopy.

Cell treatment with hyaluronidase

Cells were suspended using trypsin-EDTA (Biological Services, The Weizmann Institute), centrifuged, and re-suspended in culture medium. Hyaluronidase was added to the suspended cells to a final concentration of 500 U/ml (hyaluronidase type IV-S from bovine

testis, Sigma) or 0.15 U/ml (hyaluronidase from *S. hyalurolyticus*, Sigma). To test the potency of the enzyme, the loss of pericellular coat was assayed by a bead-exclusion test (Cohen *et al*, 2003). Incubation was performed at 37°C for 15 or 60 min, respectively. Cells were washed three times to remove residual enzyme and hyaluronan fragments. Cells were then re-suspended in serum-containing medium.

Hyaluronan labeling with QDs or colloidal gold

Cells were seeded sparsely on tissue culture dishes and allowed to adhere for 1 h, then 5 mg/ml biotinylated hyaluronan-binding protein (bHABP, Seikagaku, Japan) was added for 2 h. The cells were washed three times with medium and incubated for 30 min with 20 nM streptavidin-conjugated Qdots 655 nm (Quantum Dot Corporation, Hayward, CA), or 1:100 streptavidin-conjugated 20-nm gold particles (BBInternational, Cardiff).

Sample preparation for TIRF microscopy

Suspended cells were washed twice and re-suspended in Dulbecco's minimum essential medium without riboflavin and phenol red (Biological industries, Beit Haemek, Israel) supplemented with 30 mM HEPES (Sigma) and 15 or 0.5% fetal calf serum. The cells were then seeded on 35-mm culture plates with glass bottoms (Mattec, Ashland, MA) that were pre-incubated for 1 h with 15 or 100% fetal calf serum or with 10 μg/ml fibronectin (Sigma), and examined in an Olympus IX81 inverted microscope equipped with IX2-RFAEVA TIRF attachment (Olympus, Tokyo, Japan). Light from an argon ion laser Model I77 (lines 488 nm, 514 nm) (Spectra-Physics, Mountain View, CA) was introduced into the sample through a high numerical aperture objective lens (63 × OHR; NA 1.45, Olympus). Time-lapse movies were taken starting 1 min after seeding, using a cooled CCD camera, Quantix 57, with EEV 57-10 back-illuminated CCD chip (Photometrics, AZ). Temperature was kept at 37°C during the experiments using the Cube&Box Temperature Control System from Life Imaging Services (Reinach, Switzerland).

Sample preparation for 'wet' scanning electron microscope examination

Suspended cells were washed twice and re-suspended in α-minimum essential medium supplemented with 15% fetal calf serum. They were then seeded in QX^{TM} chambers (Quantomix Ltd, Rehovot, Israel) that were preincubated for 30 min with 25 μg/ml fibronectin (Sigma), and allowed to adhere for 5, 10, 20 or 30 min. Cells were fixed with 2% glutaraldehyde in 0.1 M cacodylate buffer, 5 mM $CaCl_2$, pH 7.2, for 30 min. They were then rinsed six times with 0.1 M cacodylate buffer, and six times with water for 5 min each. The samples were incubated with silver enhancing kit for 4 min (batch 5521, BBInternational, Cardiff), and washed extensively with water. The samples were examined in the environmental scanning electron microscope, XL 30 ESEM FEG (Philips/FEI) at 25 kV, using a low vacuum mode.

Image processing

Temporal fluorescence ratio imaging (FRIT) for comparing images of GFP fluorescence, acquired at two different time points, and fluorescence ratio imaging (FRI) for comparing two fluorophores were performed as described (Zamir *et al*, 1999). In short, images were subjected to high-pass filtration to remove background labeling and to avoid the generation of 'noisy' images resulting from the presence of low-intensity pixels in the numerator or denominator. Ratio values were calculated pixel by pixel and displayed using a spectrum scale (Zamir *et al*, 1999). In FRIT, the numerator and the denominator correspond to the earlier and later images, respectively, so that blue color indicates a new structure and a red color indicates a structure that has disappeared. In FRI, the numerator and the denominator correspond to GFP and CY3, respectively. Thus, the blue color indicates structures rich with GFP and the red indicates structures rich with CY3.

Supplementary data

Supplementary data are available at *The EMBO Journal* Online.

Acknowledgements

We thank O Zik and A Sabban (Quantomix Ltd, Rehovot, Israel) for providing us with QX^{TM} chambers, N Rosenfeld and S Itzkovitz for their help with matlab image processing, and A Florentin for preparing the paxillin–GFP fusion protein. LA is the incumbent of the Dorothy and Patrick Gorman Professorial Chair. BG is the incumbent of the E Neter Chair in Tumor and Cell Biology. ZK is the Israel Pollak professor of biophysics. This work was partly supported by the Israel Science Foundation, the Minerva Foundation, and the German Israel Foundation.

References

Albersdorfer A, Sackmann E (1999) Swelling behavior and viscoelasticity of ultathin grafted hyaluronic acid films. *Eur Phys J B* **10:** 663–672

Avnur Z, Geiger B (1981) Substrate-attached membranes of cultured cells isolation and characterization of ventral cell membranes and the associated cytoskeleton. *J Mol Biol* **153:** 361–379

Bourguignon LY, Zhu H, Shao L, Zhu D, Chen YW (1999) Rho-kinase (ROK) promotes CD44v(3, 8–10)–ankyrin interaction and tumor cell migration in metastatic breast cancer cells. *Cell Motil Cytoskelet* **43:** 269–287

Cohen M, Joester D, Geiger B, Addadi L (2004) Spatial and temporal sequence of events in cell adhesion: from molecular recognition to focal adhesion assembly. *Chembiochem* **5:** 1393–1399

Cohen M, Klein E, Geiger B, Addadi L (2003) Organization and adhesive properties of the hyaluronan pericellular coat of chondrocytes and epithelial cells. *Biophys J* **85:** 1996–2005

Critchley DR (2000) Focal adhesions—the cytoskeletal connection. *Curr Opin Cell Biol* **12:** 133–139

Curtis AS (1964) The mechanism of adhesion of cells to glass. A study by interference reflection microscopy. *J Cell Biol* **20:** 199–215

DeGrendele HC, Estess P, Picker LJ, Siegelman MH (1996) CD44 and its ligand hyaluronate mediate rolling under physiologic flow: a novel lymphocyte/endothelial cell primary adhesion pathway. *J Exp Med* **183:** 1119–1130

Draffin JE, McFarlane S, Hill A, Johnston PG, Waugh DJ (2004) CD44 potentiates the adherence of metastatic prostate and breast cancer cells to bone marrow endothelial cells. *Cancer Res* **64:** 5702–5711

Fries E, Kaczmarczyk A (2003) Inter-alpha-inhibitor, hyaluronan and inflammation. *Acta Biochim Pol* **50:** 735–742

Fujisaki T, Tanaka Y, Fujii K, Mine S, Saito K, Yamada S, Yamashita U, Irimura T, Eto S (1999) CD44 stimulation induces integrin-mediated adhesion of colon cancer cell lines to endothelial cells by up-regulation of integrins and c-Met and activation of integrins. *Cancer Res* **59:** 4427–4434

Geiger B, Bershadsky A (2002) Exploring the neighborhood: adhesion-coupled cell mechanosensors. *Cell* **110:** 139–142

Geiger B, Bershadsky A, Pankov R, Yamada KM (2001) Transmembrane crosstalk between the extracellular matrix—cytoskeleton crosstalk. *Nat Rev Mol Cell Biol* **2:** 793–805

Gileadi O, Sabban A (2003) Squid sperm to clam eggs: imaging wet samples in a scanning electron microscope. *Biol Bull* **205:** 177–179

Hanein D, Geiger B, Addadi L (1994) Differential adhesion of cells to enantiomorphous crystal surfaces. *Science* **263:** 1413–1416

Hanein D, Sabanay H, Addadi L, Geiger B (1993) Selective interactions of cells with crystal surfaces. Implications for the mechanism of cell adhesion. *J Cell Sci* **104** (Part 2)**:** 275–288

Hynes RO (1992) Integrins: versatility, modulation, and signaling in cell adhesion. *Cell* **69:** 11–25

Hynes RO (2002) Integrins: bidirectional, allosteric signaling machines. *Cell* **110:** 673–687

Iwanaga Y, Braun D, Fromherz P (2001) No correlation of focal contacts and close adhesion by comparing GFP-vinculin and fluorescence interference of Dil. *Eur Biophys J* **30:** 17–26

Izzard CS, Lochner LR (1976) Cell-to-substrate contacts in living fibroblasts: an interference reflexion study with an evaluation of the technique. *J Cell Sci* **21:** 129–159

Izzard CS, Lochner LR (1980) Formation of cell-to-substrate contacts during fibroblast motility: an interference-reflexion study. *J Cell Sci* **42:** 81–116

Johnson P, Maiti A, Brown KL, Li R (2000) A role for the cell adhesion molecule CD44 and sulfation in leukocyte–endothelial cell adhesion during an inflammatory response? *Biochem Pharmacol* **59:** 455–465

Khan AI, Kerfoot SM, Heit B, Liu L, Andonegui G, Ruffell B, Johnson P, Kubes P (2004) Role of CD44 and hyaluronan in neutrophil recruitment. *J Immunol* **173:** 7594–7601

Knudson W, Loeser RF (2002) CD44 and integrin matrix receptors participate in cartilage homeostasis. *Cell Mol Life Sci* **59:** 36–44

Laurent TC (1987) Biochemistry of hyaluronan. *Acta Otolaryngol Suppl* **442:** 7–24

Laurich C, Wheeler MA, Iida J, Neudauer CL, McCarthy JB, Bullard KM (2004) Hyaluronan mediates adhesion of metastatic colon carcinoma cells. *J Surg Res* **122:** 70–74

Lee GM, Johnstone B, Jacobson K, Caterson B (1993) The dynamic structure of the pericellular matrix on living cells. *J Cell Biol* **123:** 1899–1907

Martin KH, Slack JK, Boerner SA, Martin CC, Parsons JT (2002) Integrin connections map: to infinity and beyond. *Science* **296:** 1652–1653

Nandi A, Estess P, Siegelman M (2004) Bimolecular complex between rolling and firm adhesion receptors required for cell arrest: CD44 association with VLA-4 in T cell extravasation. *Immunity* **20:** 455–465

Petit V, Thiery JP (2000) Focal adhesions: structure and dynamics. *Biol Cell* **92:** 477–494

Ponta H, Sherman L, Herrlich PA (2003) CD44: from adhesion molecules to signalling regulators. *Nat Rev Mol Cell Biol* **4:** 33–45

Reichert WM, Truskey GA (1990) Total internal reflection fluorescence (TIRF) microscopy. I. Modelling cell contact region fluorescence. *J Cell Sci* **96** (Part 2)**:** 219–230

Savani RC, Cao G, Pooler PM, Zaman A, Zhou Z, DeLisser HM (2001) Differential involvement of the hyaluronan (HA) receptors CD44 and receptor for HA-mediated motility in endothelial cell function and angiogenesis. *J Biol Chem* **276:** 36770–36778

Shimizu KT, Woo WK, Fisher BR, Eisler HJ, Bawendi MG (2002) Surface-enhanced emission from single semiconductor nanocrystals. *Phys Rev Lett* **89:** 117401

Siegelman MH, Stanescu D, Estess P (2000) The CD44-initiated pathway of T-cell extravasation uses VLA-4 but not LFA-1 for firm adhesion. *J Clin Invest* **105:** 683–691

Toole BP (2001) Hyaluronan in morphogenesis. *Semin Cell Dev Biol* **12:** 79–87

Toole BP (2004) Hyaluronan: from extracellular glue to pericellular cue. *Nat Rev Cancer* **4:** 528–539

Turley EA, Austen L, Vandeligt K, Clary C (1991) Hyaluronan and a cell-associated hyaluronan binding protein regulate the locomotion of ras-transformed cells. *J Cell Biol* **112:** 1041–1047

Zaidel-Bar R, Cohen M, Addadi L, Geiger B (2004) Hierarchical assembly of cell–matrix adhesion complexes. *Biochem Soc Trans* **32:** 416–420

Zamir E, Geiger B (2001) Molecular complexity and dynamics of cell–matrix adhesions. *J Cell Sci* **114:** 3583–3590

Zamir E, Katz BZ, Aota S, Yamada KM, Geiger B, Kam Z (1999) Molecular diversity of cell–matrix adhesions. *J Cell Sci* **112** (Part 11)**:** 1655–1669

Zamir E, Katz M, Posen Y, Erez N, Yamada KM, Katz BZ, Lin S, Lin DC, Bershadsky A, Kam Z, Geiger B (2000) Dynamics and segregation of cell–matrix adhesions in cultured fibroblasts. *Nat Cell Biol* **2:** 191–196

Zimmerman E, Geiger B, Addadi L (2002) Initial stages of cell–matrix adhesion can be mediated and modulated by cell–surface hyaluronan. *Biophys J* **82:** 1848–1857